Supplemental Data. Ye et al. (2009). Arabidopsis formin3 directs the formation of actin cables and polarized growth in pollen tubes.

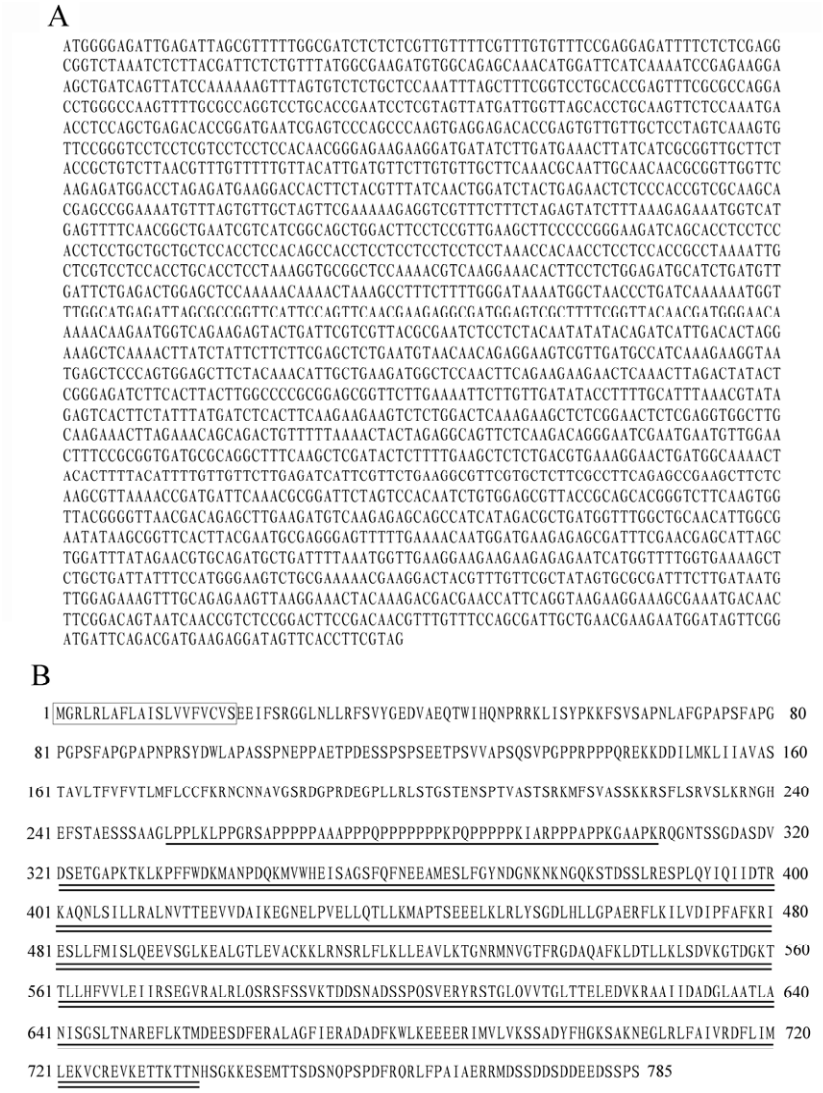

Supplemental Figure 1. The coding region nucleotide sequence of *AFH3* and its encoded amino acid sequence.

(A) The coding region nucleotide sequence of *AFH3*..

(B) The amino acid sequence of AFH3. The signal peptide is indicated by an open box. The FH1 domain which contains a poly-proline rich motif, is underlined. The FH2 domain is double underlined.

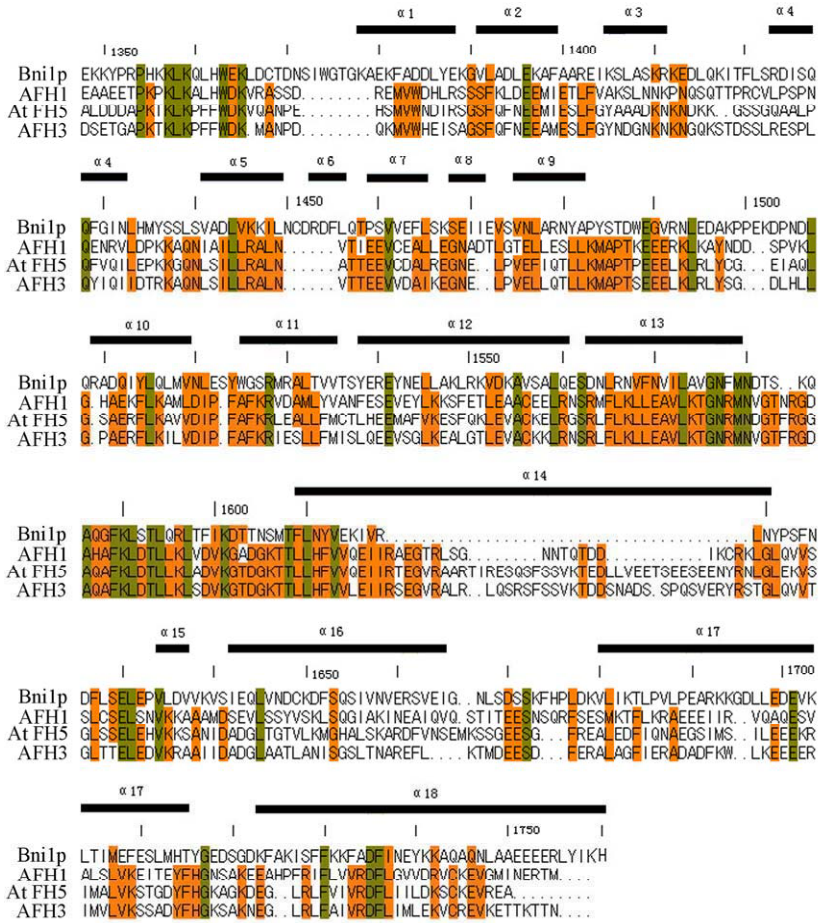

Supplemental Figure 2. The FH2 domain of AFH3 is highly conserved compared it with FH2 domains of other formins.

Sequence alignment of the FH2 domain of AFH3 with the equivalent domain of budding yeast Bni1p, AFH1, and At FH5, based on the structure of FH2 domain of Bni1p (Xu et al., 2004). Multiple sequence alignment was done with DNAMAN6.0.40. Superimposition with the secondary structures extracted from the Bni1p crystal structure (Protein Data Bank ID 1UX5) was done with EsPript (http://espript.ibcp.fr/ESPript/ESPript/). Numbering is based on the Bni1p crystal structure (1UX5). Helices are represented with rectangles above the sequence. A

hundred percent identity of amino acid was marked with light green, and 75% identity of amino acid was marked with orange.

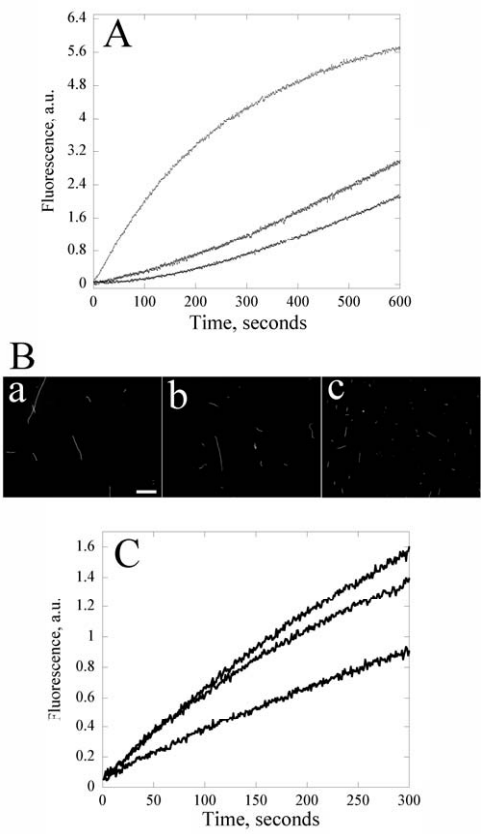

Supplemental Figure 3. AFH3 FH2 has hardly detectable actin nucleation activity and does not cap barbed ends of actin filaments.

(A) AFH3 FH2 has hardly detectable actin nucleation activity. The curve from bottom to top is: Actin alone (2 μM); Actin plus 500 nM AFH3 FH2; Actin plus 500 nM AFH3 FH1FH2.

(B) Micrographs of actin filaments. (a) Actin alone; (b) Actin plus 600 nM AFH3 FH2; (c) Actin plus 300 nM AFH3 FH1FH2. Bar=10 μm for (a)-(c).

(C) AFH3 FH2 does not cap barbed ends of actin filaments. Preformed actin filaments (0.8 μM) were incubated with various concentrations of AFH3 FH1FH2 before the

addition of 1 μM pyrene-actin monomers. The curve from top to bottom is: addition of 1 μM G-actin alone; addition of 1 μM G-actin before pre-incubation with 1 μM AFH3 FH2; addition of 1 μM G-actin before pre-incubation with 1 μM AFH3 FH1FH2.

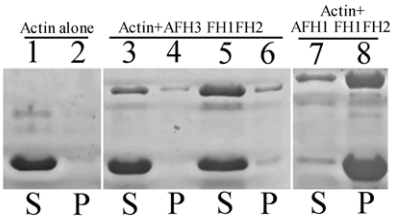

Supplemental Figure 4. AFH3 FH1FH2 does not bundle actin filaments.

A low-speed co-sedimentation assay was employed to test whether AFH3 FH1FH2 bundles actin filaments. A mixture of 3 μM F-actin in the absence or presence of formin proteins was centrifuged at 13,500 g for 30 min at 4°C. The resulting supernatants (S) and pellets (P) were subjected to SDS-PAGE and Coomassie-stained. The samples include: lane 1, actin alone supernatant; lane 2, actin alone pellet; lane 3, actin plus 500 nM AFH3 FH1FH2 supernatant; lane 4 actin plus 500 nM AFH3 FH1FH2 pellet; lane 5 actin plus 1000 nM AFH3 FH1FH2 supernatant; lane 6, actin plus 1000 nM AFH3 FH1FH2 pellet; lane 7, actin plus 1000 nM AFH1 FH1FH2 supernatant; lane 8, actin plus 1000 nM AFH1FH1FH2 pellet.

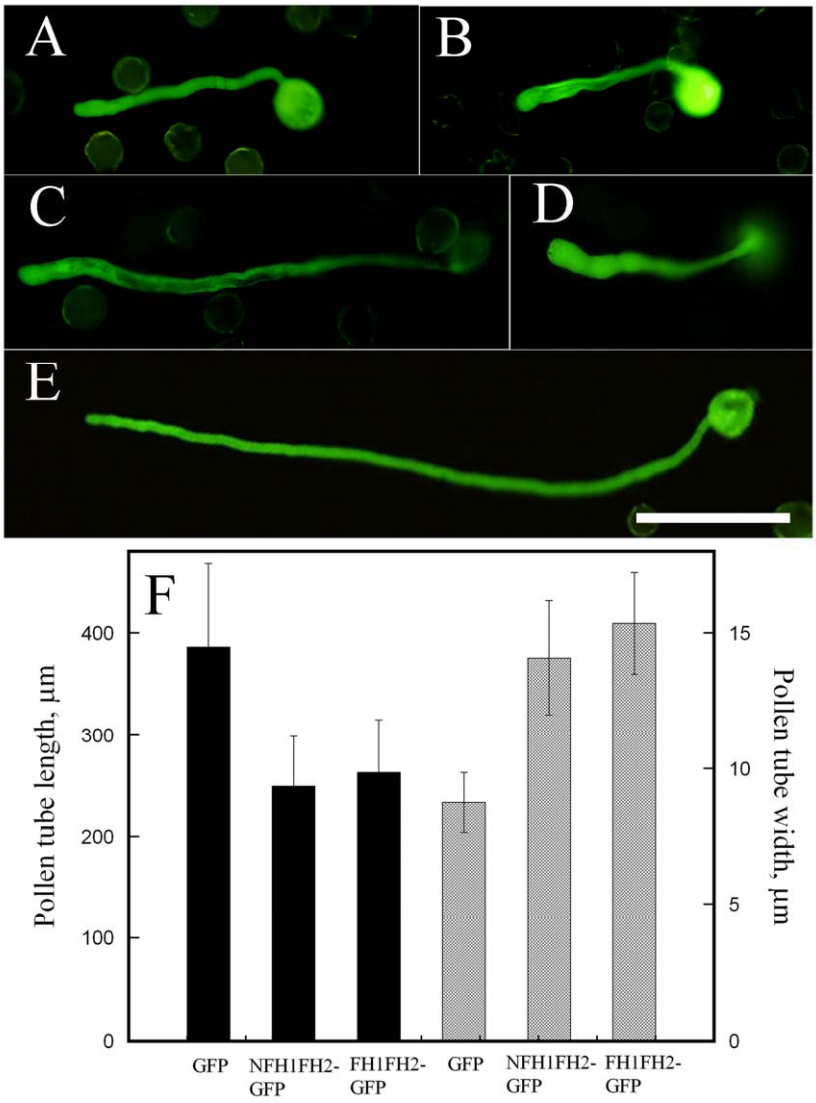

Supplemental Figure 5. Overexpression of both NΔFH1FH2-GFP and ΔFH1FH2-GFP arrest pollen tube growth and caused pollen tube swelling.

(A) and (B) pollen tubes transformed by Lat52:NΔFH1FH2 -GFP (1 µg); Typically, more than 80% of all transformed pollen tubes displayed a phenotype similar to that shown in (A) and less than 15% of transformed pollen tubes displayed a phenotype similar to that shown in (B).

(C) and (D) pollen tubes typical of those transformed by Lat52: ΔFH1FH2-GFP (1 μg). More than 75% of all transformed pollen tubes displayed a phenotype similar to that shown in (C) and about 20% of transformed pollen tubes displayed a phenotype similar to that shown in (D). The width of the pollen tube correlates with the expression level; the stronger the fluorescence, the wider the pollen tube.

(E) A control pollen tube transformed by Lat52:GFP (1 μg); Bar=50 μm in (A) to (E).

(F)Average length and width of the pollen tubes transformed by Lat52:GFP, Lat52: NΔFH1FH2-GFP and Lat52: ΔFH1FH2-GFP. Average pollen tube length (±S.D.) and width for more than 35 transformed tubes from each sample were plotted.

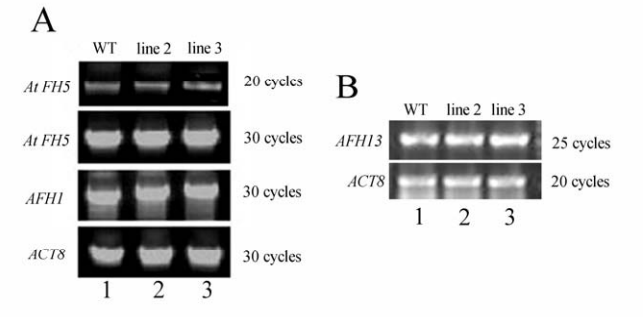

Supplemental Figure 6. The transcript level of *AFH1, At FH5* and *AFH13* does not decrease in AFH3 RNAi flowers.

Total RNA was isolated from Col and AFH3 RNAi mutant flowers, and subjected to RT-PCR analyses using primers specific for *AFH1* and At *FH5*. *ACT8* was used as a positive internal control. (A). Expression level of *AFH1* and At *FH5* in AFH3 RNAi flowers. Lane 1, RNA of Columbia wild type subjected to RT treatment; Lane 2 and Lane 3, RNA of AFH3 RNAi line 2 and line 3 subjected to RT treatment, respectively. (B). Expression level of *AFH13* in AFH3 RNAi flowers. Lane 1, RNA of Columbia wild type subjected to RT treatment; Lane 2 and Lane 3, RNA of AFH3 RNAi line 2 and line 3 subjected to RT treatment, respectively.

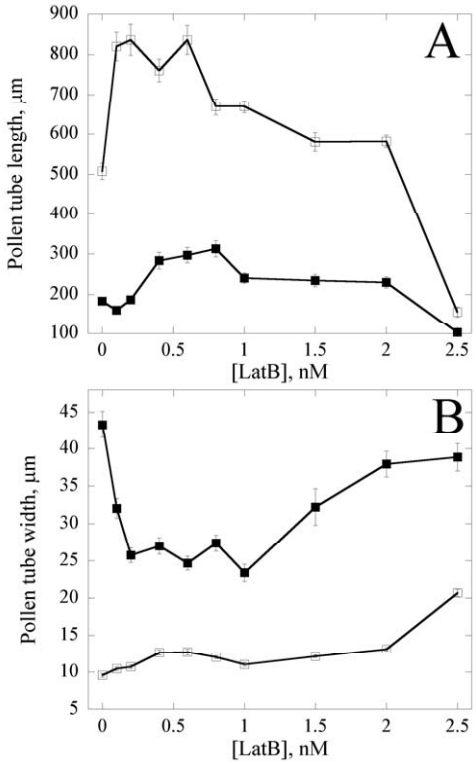

Supplemental Figure 7. LatB partially suppress the phenotype of AFH3 RNAi pollen tubes.

Wild-type and AFH3 RNAi pollen tubes (line 3) were germinated in germination medium containing various concentrations of LatB. The length and width of pollen tubes were measured after 5 h of germination. (A) Plot of average length (±S.E.) of pollen tubes (n=30) versus LatB concentration. Wild type (empty squares), AFH3 RNAi (filled squares).

(B) Plot of average width (±S.E.) of pollen tubes (n=30) versus LatB concentration. Wild type (empty squares), AFH3 RNAi (filled squares).

Supplemental Methods

Low speed co-sedimentation assay

Low speed cosedimentation assay was carried out roughly according to (Huang et al., 2005). In a 100-µl reaction volume, 3 µM actin alone or with AFH1 FH1FH2 or AFH3 FH1FH2 were incubated in 1×F-buffer (10×stock: 50mM Tris-HCl, pH 7.5, 5 mM DTT, 5 mM ATP, 1 M KCl, 50 mM $MgCl_2$). After incubation for 1 h at 22°C, samples were centrifuged at 13,500 g for 30 min at 4°C. Equal amounts of pellet and supernatant samples were separated by SDS-PAGE.

Supplemental References

Huang, S., Robinson, R.C., Gao, L.Y., Matsumoto, T., Brunet, A., Blanchoin, L., and Staiger, C.J. (2005). Arabidopsis VILLIN1 generates actin filament cables that are resistant to depolymerization. Plant Cell 17, 486-501.